

Electronic Supplementary Material (ESI)

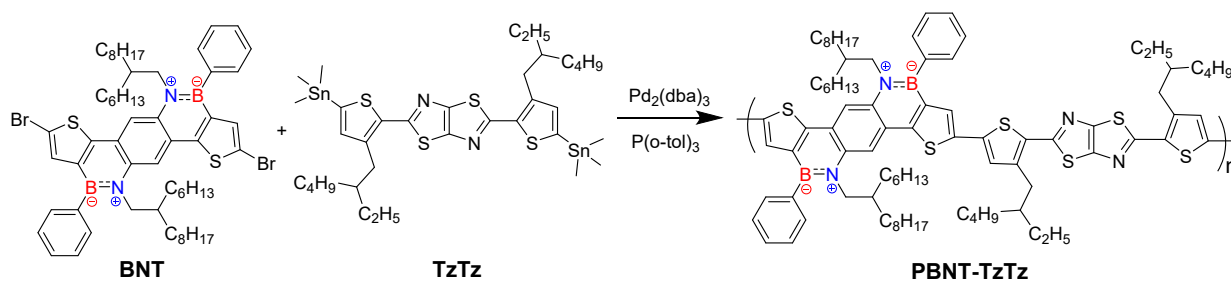
## Supplemental information

### High-Efficiency Organic Solar Cells Processed from Real Green Solvent

Shuting Pang, Zhili Chen, Junyu Li, Yuting Chen, Zhitian Liu, Hongbin Wu, Chunhui Duan,\*  
Fei Huang, and Yong Cao

#### 1. Polymer synthesis

**General information:** The synthesis route of the polymer PBNT-TzTz is shown in Scheme S1. The monomers BNT and TzTz were synthesized according to the procedures reported in literatures.<sup>1,2,3</sup> Pd<sub>2</sub>(dba)<sub>3</sub> was purchased from Strem. The other chemicals and solvents were purchased from commercial sources (Innochem, Energy Chemical, or Acros) and used as received unless otherwise indicated. Y6, Y6-BO and PTQ10 were purchased from eFlexPV Limited (China). D18 was purchased from Derthon OPV Co Ltd. L8-BO was purchased from Hyper Inc.



**Scheme S1.** The synthetic route of PBNT-TzTz.

**Polymerization of PBNT-TzTz:** In the degassed solution containing the monomer BNT (210.1 mg, 0.2 mmol) and TzTz (171.3 mg, 0.2 mmol) in anhydrous *o*-xylene (3.6 ml) and *N,N*-dimethylformamide (0.4 ml), Pd<sub>2</sub>(dba)<sub>3</sub> (3.7 mg, 0.004 mmol) and P(*o*-tol)<sub>3</sub> (9.7 mg, 0.032 mmol) were added under nitrogen protection. Then the mixture was stirred at 110 °C for 48 hours. After that, 2-(tributylstannyl)thiophene and 2-bromothiophene were sequentially added

to the reaction with 2 hours interval. After cooling to room temperature, the reaction mixture was precipitated in methanol and filtered through a Soxhlet thimble. The precipitation was subjected to Soxhlet extraction with methanol, acetone, hexane, dichloromethane, chloroform, and chlorobenzene sequentially under argon protection. The chlorobenzene fraction was concentrated under reduced pressure and precipitated in methanol to obtain the polymer PBNT-TzTz (Yield = 93%).  $M_n = 42$  kDa,  $D_M = 2.4$ .

## 2. Measurements and characterization

**Gel permeation chromatography (GPC):** The molecular weight of the polymer was determined by Agilent Technologies PL-GPC 220 high-temperature chromatography in 1,2,4-trichlorobenzene at 140 °C using a calibration curve of polystyrene standards.

**Thermogravimetric analysis (TGA):** The TGA measurement was carried out with a NETZSCH (TG209F3) apparatus at a heating rate of 20 °C min<sup>-1</sup> under nitrogen atmosphere.

**Differential scanning calorimetry (DSC):** The DSC measurement was performed on a NETZSCH (DSC200F3) apparatus with a heating/cooling rate of 10/20 °C min<sup>-1</sup> for the first cycle and 10/40 min<sup>-1</sup> for the second cycle under nitrogen atmosphere.

**Measurements of dielectric constant:** The dielectric constants of the materials were determined by the capacitance–voltage ( $C-V$ ) measurements with a device structure of ITO/PEDOT:PSS/polymer film (150 nm)/Al. First, PEDOT:PSS (CLEVIOS™ P VP AI 4083) was spin-coated on top of a cleaned ITO and annealed in air at 150 °C for 15 minutes to form a  $\approx 40$  nm layer. Subsequently, the polymer film with the thickness of 150 nm was formed by spin-coating the solution of PBNT-TzTz or PBDT-TzTz in chloroform on top of the PEDOT:PSS layer. After that, a 100 nm Al layer was deposited by thermal evaporation through a shadow mask in a vacuum chamber at a pressure of  $5 \times 10^{-6}$  Torr. The  $C-V$  measurements of the molecules were performed using a HP 4192A LCR meter by sweeping the voltage from –30 to 10 V at room temperature, with a ramping rate of 0.5 V s<sup>-1</sup> and 30 mV of oscillator levels. The measurements were performed under the frequency from  $1 \times 10^3$  to  $1 \times 10^6$  Hz. The relative

dielectric constants ( $\epsilon_r$ ) were calculated from the equation of  $\epsilon_r = Cd/\epsilon_0A$ , where  $C$  is the capacitance,  $d$  is the thickness of the polymer film,  $\epsilon_0$  is the permittivity of free space,  $A$  is the device area (0.0516 cm<sup>2</sup>).

**UV–vis–NIR absorption spectra:** UV–vis–NIR absorption spectra of the polymers and non-fullerene acceptor in chlorobenzene solutions and as thin films were recorded on a SHIMADZU UV-3600 spectrophotometer. The concentration of diluted solution was  $1.0 \times 10^{-5}$  M, and the films were prepared by spin coating their solutions on glass substrates.

**Square wave voltammetry (SWV):** SWV measurements were conducted on a CHI600D electrochemical workstation in a solution of tetrabutylammonium hexafluorophosphate (Bu<sub>4</sub>NPF<sub>6</sub>, 0.1 M) in acetonitrile at a scan rate of 50 mV s<sup>-1</sup>. A platinum electrode coated with the sample film, a platinum wire, and an Ag/AgCl electrode were used as working electrode, counter electrode, and reference electrode, respectively. The highest occupied molecular orbital (HOMO) and lowest unoccupied molecular orbital (LUMO) energy levels were calculated by  $E_{\text{HOMO/LUMO}} = -(E_{\text{ox/red}} + 5.13 - E_{\text{Fc/Fc}^+})$ .<sup>4,5</sup>

**Density functional theory (DFT):** The geometry was fully optimized at the B3LYP/ 6-31+G\* level of theory by the absence of imaginary frequencies. The long alkyl chains were replaced by methyl groups. All calculations were carried out with the Gaussian 09 software.<sup>6</sup>

**Steady-state photoluminescence (PL) quenching measurements:** The PL quenching measurements were conducted on a Shimadzu RF-6000 spectrometer.

**Atomic force microscopy (AFM):** The AFM images were obtained by Bruker Multimode 8 Microscope AFM in tapping mode.

**Transmission electron microscopy (TEM):** The TEM images were collected from JEM-2100F transmission electron microscope operated at 200 kV.

**Grazing incidence wide-angle X-ray scattering (GIWAXS):** 2D-GIWAXS experiments were carried out on a GANESHA 300XL+ system from JJ X-ray. The instrument is equipped with a Pilatus 300K detector, with pixel size of  $172 \times 172$   $\mu\text{m}$ . The X-ray source is a Genix 3D

Microfocus Sealed Tube X-Ray Cu-source with integrated Monochromator (multilayer optic “3D version” optimized for SAXS) (30 W). The wavelength used is  $\lambda = 1.5418 \text{ \AA}$ . The detector moves in a vacuum chamber with sample-to-detector distance varied between 0.115 m and 1.47 m depending on the configuration used, as calibrated using silver behenate ( $d_{001} = 58.380 \text{ \AA}$ ). The minimized background scattering plus high-performance detector allows for a detectable  $q$ -range varying from  $3 \times 10^{-3}$  to  $3 \text{ \AA}^{-1}$  (0.2 to 210 nm). The sample was placed vertically on the goniometer and tilted to a glancing angle of  $0.2^\circ$  with respect to the incoming beam. A small beam was used to get a better resolution. The primary slits have a size of 0.3 (horizontal)  $\times$  0.5 mm (vertical), and the guard slits have a size of 0.1 (horizontal)  $\times$  0.3 (horizontal) mm. The accumulation time was 2 hours for each measurement. In-plane and out-of-plane line-cut profiles were obtained using SAXSGUI program.

### 3. Device fabrication and characterization

**The fabrication of solar cells:** The substrates with indium tin oxide (ITO) were cleaned by detergent, sonicated in deionized water and isopropanol, subsequently. After that, the clean substrates were dried in blast oven at  $70 \text{ }^\circ\text{C}$ . The ITO substrates were subjected to oxygen plasma for 5 minutes. An aqueous solution of PEDOT:PSS (CLEVIOS<sup>TM</sup> P VP AI 4083) was spin-casted onto the ITO surface at 3000 rpm for 30 seconds, followed by drying at  $150 \text{ }^\circ\text{C}$  for 15 minutes in air. The substrates were then transferred into a nitrogen-filled glove box. The active layer was fully optimized in terms of D/A ratio, spin-coating rate, solvent composition, and thermal annealing. For the optimal PBNT-TzTz:Y6-BO device, the polymer and Y6-BO were dissolved in a mixed solution of anisole and LM at the donor concentration of  $7 \text{ mg mL}^{-1}$ . The active layers were spin-coated on substrates at 2500 rpm to give a thickness of 100 nm. Afterwards, an electron transport layer of PNDIT-F3N was spin-coated from a solution ( $0.5 \text{ mg mL}^{-1}$ ) at a speed of 2000 rpm for 30 seconds. Finally, a 100 nm Ag was deposited by thermal evaporation in a vacuum chamber at a pressure of  $5 \times 10^{-6}$  Torr with a shadow mask.

**Photovoltaic performance:** The photovoltaic performance of the solar cells were measured under AM1.5G irradiation ( $100 \text{ mW cm}^{-2}$ ) derived from a class solar simulator (Enlitech, Taiwan), which was calibrated by a China General Certification Center-certified reference single-crystal silicon cell (Enlitech). The current density–voltage ( $J$ – $V$ ) curves were recorded with a Keithley 2400 source meter.

**External quantum efficiencies (EQEs):** The EQE spectra were measured by a QE system (QE-R3011, Enlitech) with the light intensity calibrated by a standard single-crystal silicon photovoltaic cell (Enlitech).

**Light-intensity dependence:** The light-intensity dependence measurements were carried out in illumination with a photon flux between  $10$ – $100 \text{ mW cm}^{-2}$ , which was calibrated by a standard single-crystal silicon solar cell (Enlitech). The current density and voltage were recorded with a Keithley 2400 source meter.

**Fabrication and characterization of single-carrier devices:** Single-carrier devices were fabricated to measure hole and electron mobility by using the space-charge-limited current (SCLC) method. The device structures of the hole-only and electron-only devices are ITO/PEDOT:PSS (40 nm)/active layer (100 nm)/MoO<sub>x</sub> (10 nm)/Ag (100 nm) and ITO/ZnO (40 nm)/active layer (100 nm)/PFN-Br (10 nm)/Ag (100 nm), respectively. The dark current densities of the devices were measured by applying a voltage between 0 and 5 V using a computer-controlled Keithley 2400 source meter under a nitrogen atmosphere. The data were analyzed according to the Mott–Gurney law that considers a Poole–Frenkel-type dependence

of mobility on the electric field, given by  $J = \frac{9}{8\epsilon_r\epsilon_0\mu_0} \exp(0.89\gamma\sqrt{V/d})$ , where  $\epsilon_0$  is the permittivity of free space,  $\epsilon_r$  is the dielectric constant which is assumed to be 3 for organic semiconductors,  $\mu_0$  is the zero-field mobility,  $V$  is the voltage drop across the device,  $d$  is the film thickness of the active layer, and  $\gamma$  is a parameter that describes the strength of the field-dependence effect. The applied voltage is used without correcting for series resistance or built-

in voltage, which offers the best fitting of the experimental data following the protocol reported in literature.<sup>7</sup> The hole and electron mobilities are extracted with the fit parameters at an electric field ( $E$ ) of  $1 \times 10^5 \text{ V cm}^{-1}$  by the Murgatroyd equation  $\mu = \mu_0 \exp(\gamma\sqrt{E})$ .

**Transient Optoelectronic Measurements:** For TPV measurements, the solar cells were first illuminated by a halogen lamp with  $100 \text{ mW cm}^{-2}$  illumination to reach working condition. A set of neutral optical filter were utilized to produce 0.01–1 sun illumination. Perturbed charge carriers were then generated by a 532 nm laser pulse from a Nd:YAG pulse laser (Q-smart 100 of Quantel). The TPV signals were monitored by a Tektronix DPO4014 oscilloscope with high input impedance option to achieve open-circuit condition. For TPC measurements, the solar cells were in series with a  $50 \Omega$  load resistor. The voltage transient across the resistor was recorded by the oscilloscope under the same illumination and laser perturbation. The transient is translated into a current transient by Ohm's law.

#### 4. Additional figures and tables

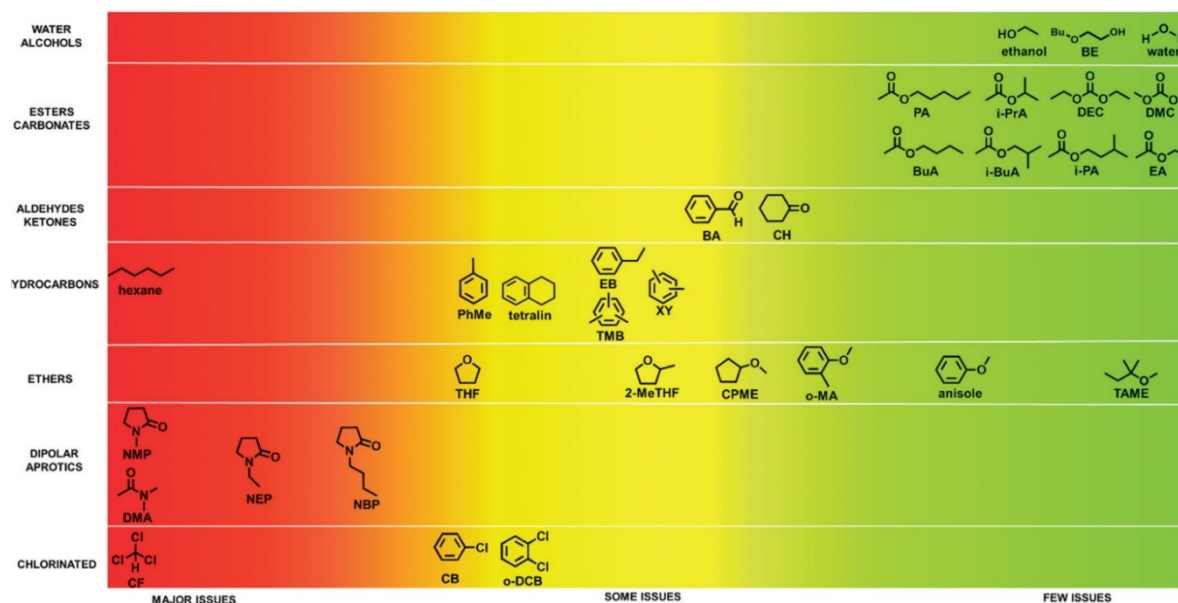


**Fig. S1.** Ranking of the solvents investigated for OSCs processing based on the overall greenness criterion. Reproduced with permission.<sup>8</sup> Copyright 2020, the Royal Society of Chemistry.

**Table S1.** CHEM21 solvent guide of common solvents. Reproduced with permission.<sup>9</sup> Copyright 2016, the Royal Society of Chemistry.

**Table 7** CHEM21 solvent guide of "classical" solvents

Family	Solvent	BP (°C)	FP (°C)	Worst H3xx <sup>d</sup>	H4xx	Safety score	Health score	Env. score	Ranking by default	Ranking after discussion <sup>b</sup>
Water	Water	100	na	None	None	1	1	1	Recommended	Recommended
Alcohols	MeOH	65	11	H301	None	4	7	5	Problematic	Recommended
	EtOH	78	13	H319	None	4	3	3	Recommended	Recommended
	i-PrOH	82	12	H319	None	4	3	3	Recommended	Recommended
	n-BuOH	118	29	H318	None	3	4	3	Recommended	Recommended
	t-BuOH <sup>c</sup>	82	11	H319	None	4	3	3	Recommended	Recommended
	Benzyl alcohol	206	101	H302	None	1	2	7	Problematic	Problematic
	Ethylene glycol	198	116	H302	None	1	2	5	Recommended	Recommended
Ketones	Acetone	56	-18	H319	None	5	3	5	Problematic	Recommended
	MEK	80	-6	H319	None	5	3	3	Recommended	Recommended
	MIBK	117	13	H319	None	4	2	3	Recommended	Recommended
	Cyclohexanone	156	43	H332	None	3	2	5	Recommended	Problematic
Esters	Methyl acetate	57	-10	H302	None	5	3	5	Problematic	Problematic
	Ethyl acetate	77	-4	H319	None	5	3	3	Recommended	Recommended
	i-PrOAc	89	2	H319	None	4	2	3	Recommended	Recommended
	n-BuOAc	126	22	H336	None	4	2	3	Recommended	Recommended
Ethers	Diethyl ether	34	-45	H302	None	10	3	7	Hazardous	HH
	Diisopropyl ether	69	-28	H336	None	9	3	5	Hazardous	Hazardous
	MTBE	55	-28	H315	None	8	3	5	Hazardous	Hazardous
	THF	66	-14	H351	None	6	7	5	Problematic	Problematic
Me-THF	80	-11	H318	None	6	5	3	Problematic	Problematic	
1,4-Dioxane	101	12	H351	None	7	6	3	Problematic	Hazardous	
Anisole	154	52	None	None	4	1	5	Problematic	Recommended	
Hydrocarbons	DME	85	-6	H360	None	7	10	3	Hazardous	Hazardous
	Pentane	36	-40	H304	H411	8	3	7	Hazardous	Hazardous
	Hexane	69	-22	H361	H411	8	7	7	Hazardous	Hazardous
	Heptane	98	-4	H304	H410	6	2	7	Problematic	Problematic
	Cyclohexane	81	-17	H304	H410	6	3	7	Problematic	Problematic
	Me-cyclohexane	101	-4	H304	H411	6	2	7	Problematic	Problematic
	Benzene	80	-11	H350	None	6	10	3	Hazardous	HH
	Toluene	111	4	H351	None	5	6	3	Problematic	Problematic
Xylenes	140	27	H312	None	4	2	5	Problematic	Problematic	
Halogenated	DCM	40	na	H351	None	1	7	7	Hazardous	Hazardous
	Chlorotorm	61	na	H351	None	2	7	5	Problematic	HH
	CCl <sub>4</sub>	77	na	H351	H420	2	7	10	Hazardous	HH
	DCE	84	13	H350	None	4	10	3	Hazardous	HH
Chlorobenzene	132	29	H332	H411	3	2	7	Problematic	Problematic	
Aprotic polar	Acetonitrile	82	2	H319	None	4	3	3	Recommended	Problematic
	DMF	153	58	H360	None	3	9	5	Hazardous	Hazardous
	DMAc	166	70	H360	None	1	9	5	Hazardous	Hazardous
	NMP	202	96	H360	None	1	9	7	Hazardous	Hazardous
	DMPU	246	121	H361	None	1	6	7	Problematic	Problematic
	DMSO <sup>c</sup>	189	95	None	None	1	1	5	Recommended	Problematic
	Sulfolane <sup>c</sup>	287	177	H360	None	1	9	7	Hazardous	Hazardous
	HMPA	>200	144	H350	None	1	9	7	Hazardous	HH
Miscellaneous	Nitromethane	101	35	H302	None	10	2	3	Hazardous	HH
	Methoxy-ethanol	125	42	H360	None	3	9	3	Hazardous	Hazardous
	Carbon disulfide	46	-30	H361	H412	9	7	7	Hazardous	HH
Acids	Formic acid	101	49	H314	None	3	7	3	Problematic	Problematic
	Acetic acid	118	39	H314	None	3	7	3	Problematic	Problematic
Amines	Ac <sub>2</sub> O	139	49	H314	None	3	7	3	Problematic	Problematic
	Pyridine	115	23	H302	None	4	2	3	Recommended	Hazardous
	TEA	89	-6	H314	None	6	7	3	Problematic	Hazardous

**Table S2.** Sanofi solvent guide of common solvents. Reproduced with permission.<sup>10</sup> Copyright 2013, the Royal Society of Chemistry.

Solvents Guide	ETHERS: OVERVIEW					
Name	Overall ranking	ICH limit (ppm)	Occ. health	Safety	Environment	Other concern
<a href="#">Diethyl ether</a>	Banned	5000	OEBV2	SHB5	EHB2	Peroxides, VOC
<a href="#">Diisopropyl ether</a>	Substitution advisable	Not listed	OEBV2	SHB5	EHB3	Peroxides
<a href="#">Dibutyl ether</a>	Substitution advisable	Not listed	OEBV2	SHB5	EHB3	Peroxides, odor
<a href="#">THF</a>	Substitution advisable	720	OEBV3 Sk	SHB4	EHB2	VOC, miscible with water, peroxides
<a href="#">Methyl-THF</a>	Recommended	Not listed	OEBV2	SHB4	EHB3	Peroxides, cost
<a href="#">Dioxane</a>	Substitution requested	380	OEBV3 Sk	SHB5	EHB2	Miscible with water, peroxides
<a href="#">Anisole</a>	Recommended	5000	OEBV2	SHB3	EHB2	Odor
<a href="#">MTBE</a>	Substitution advisable	5000	OEBV3 Sk	SHB5	EHB3	VOC
<a href="#">ETBE</a>	Substitution requested	Not listed	OEBV4	SHB5	EHB3	Peroxides, lack of data
<a href="#">CPME</a>	Substitution requested	Not listed	OEBV3	SHB5	EHB3	Peroxides, one supplier only
<a href="#">Dimethoxy ethane</a>	Substitution requested	100	OEBV4 G2	SHB4	EHB2	CMR (R1B), peroxides
<a href="#">Diglyme</a>	Substitution requested	Not listed	OEBV4 G2	SHB4	EHB2	CMR (R1B), peroxides
<a href="#">Diethoxymethane</a>	Substitution requested	Not listed	OEBV4	SHB5	Not available	Reactive, considered as CMR

**Table S3.** GlaxoSmithKline solvent guide of common solvents. Reproduced with permission.<sup>11</sup> Copyright 2011, the Royal Society of Chemistry.

Classification	Solvent <small>click on solvent name for hyperlink to more detail</small>	Cas number	Melting point °C	Boiling point °C	Waste	Environmental Impact	Health	Flammability & Explosio	Reactivity/Stability	Life Cycle Score	Legislation Flag	EHS Red Flag
Hydrocarbon	<a href="#">cis-Decalin</a>	493-01-6	-43	196	7	3	7	6	7	7		
	<a href="#">ISOPAR G</a>	64742-48-9	-60	163	8	2	9	6	10			
	<a href="#">Isooctane</a>	540-84-1	-107	99	6	4	8	3	10	7		
	<a href="#">Methyl cyclohexane</a>	108-87-2	-127	101	6	5	8	3	10	7		
	<a href="#">Cyclohexane</a>	110-82-7	7	81	5	5	7	2	10	7		
	<a href="#">Heptane</a>	142-82-5	-91	98	6	3	8	3	10	7		
	<a href="#">Pentane</a>	109-66-0	-130	36	5	6	8	2	10	7		
	<a href="#">Methylcyclopentane</a>	96-37-7	-142	72	6	4	5	2	9	7		
	<a href="#">2-Methylpentane</a>	107-83-5	-153	60	5	4	7	2	10	7		
	<a href="#">Hexane</a>	110-54-3	-95	69	5	3	4	2	10	7		
	<a href="#">Petroleum spirit</a>	8032-32-4	-73	55	6	2	2	3	10	7		
	<a href="#">Di(ethylene glycol)</a>	111-46-6	-10	246	6	8	7	9	9	8		
	<a href="#">Ethoxybenzene</a>	103-73-1	-29	170	8	4	7	10	10			
	<a href="#">Tri(ethylene glycol)</a>	112-27-6	-7	285	6	8	6	10	9	7		
<a href="#">Sulfolane</a>	126-33-0	28	282	5	9	6	10	10				
<a href="#">DEG monobutyl ether</a>	112-34-5	-68	231	6	7	7	9	6	7			
<a href="#">Anisole</a>	100-66-3	-38	154	6	6	7	7	6	5			
<a href="#">Diphenyl ether</a>	101-84-8	27	258	8	5	4	8	6				
<a href="#">Dibutyl ether</a>	142-96-1	-95	140	7	7	4	5	5	4			
<a href="#">t-Amyl methyl ether</a>	994-05-8	-80	86	5	5	5	5	9	8			
<a href="#">t-Butylmethyl ether</a>	1634-04-4	-109	55	4	5	5	3	9	8			
<a href="#">Cyclopentyl methyl ether</a>	5614-37-9	-140	106	6	4	4	5	8	4			
<a href="#">t-Butyl ethyl ether</a>	637-92-3	-74	70	5	5	4	4	9	8			
<a href="#">2-Methyltetrahydrofuran</a>	96-47-9	-137	78	4	5	4	3	6	4			
<a href="#">Diethyl ether</a>	60-29-7	-116	35	4	4	4	5	2	4	6		
<a href="#">Bis(2-methoxyethyl) ether</a>	111-96-6	-68	162	4	5	2	8	4	6			
<a href="#">Dimethyl ether</a>	115-10-6	-141	-25	3	5	7	1	4	7			
<a href="#">1,4-Dioxane</a>	123-91-1	12	102	3	4	4	4	5	6			
<a href="#">Tetrahydrofuran</a>	109-99-9	-108	65	3	5	6	3	4	4			
<a href="#">1,2-Dimethoxyethane</a>	110-71-4	-58	85	4	5	2	4	4	7			
<a href="#">Diisopropyl ether</a>	108-20-3	-86	68	4	3	8	1	1	9			
<a href="#">Dimethylpropylene urea</a>	7226-23-5	-23	247	7	7	4	9	7	3			
<a href="#">Dimethyl sulphoxide</a>	67-68-5	19	189	5	5	7	9	2	6			
<a href="#">Formamide</a>	75-12-7	3	220	4	7	2	10	8	8			
<a href="#">Dimethyl formamide</a>	68-12-2	-61	153	4	6	2	9	9	7			
<a href="#">N-Methylformamide</a>	123-39-7	-4	200	4	6	2	10	10	7			
<a href="#">N-Methyl pyrrolidone</a>	872-50-4	-24	202	5	6	3	9	8	4			
<a href="#">Propanenitrile</a>	107-12-0	-93	97	3	6	4	6	9				
<a href="#">Dimethyl acetamide</a>	127-19-5	-20	165	5	6	2	10	8	2			
<a href="#">Acetonitrile</a>	75-05-8	-45	82	2	6	6	6	10	3			

**Table S4.** The reported evaluation coefficient, HSP parameters and boiling point of solvents.

NO.	Solvent	Health score <sup>a</sup>	Safety score <sup>a</sup>	Environment score <sup>a</sup>	Ranking by defined	$\delta_D$	$\delta_P$	$\delta_H$	b.p.
1	CF	2	7	5	Highly hazardous	17.8	3.1	5.7	61 °C
2	CB	3	2	7	Problematic	19.0	4.3	2.0	132 °C
4	Toluene	6	6	3	Problematic	18.0	1.4	2.0	110 °C
5	<i>o</i> -Xylene	4	2	5	Problematic	18.0	2.6	2.8	144 °C
6	THF	7	6	5	Problematic	16.8	5.7	8.0	66 °C
7	Me-THF	5	6	3	Problematic	16.4	4.7	4.6	80 °C
8	Water	1	1	1	Recommend	15.5	16.0	42.3	100 °C
9	Ethyl alcohol	4	3	3	Recommend	15.8	8.8	19.4	78 °C
10	Anisole	2	3	2	Recommend	17.8	4.4	6.9	155 °C

<sup>a</sup>The value represents the hazard level.

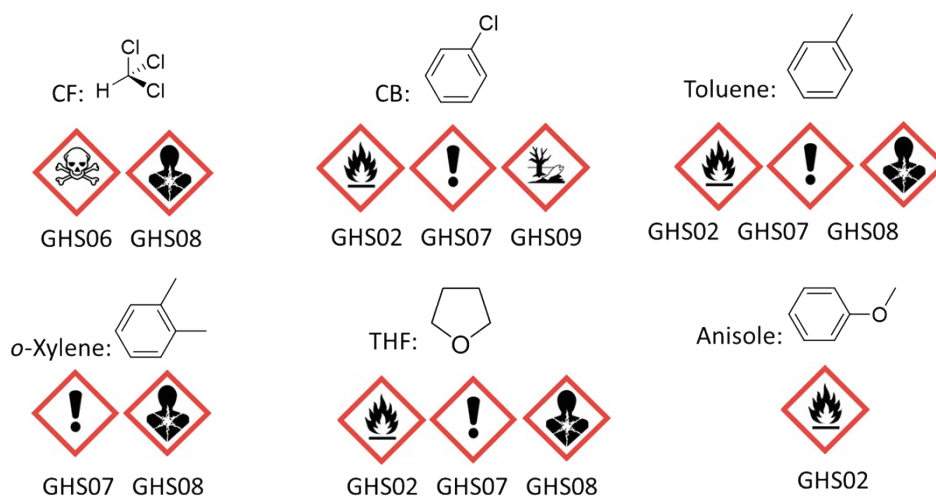


**Fig. S2.** GHS labels of representative solvents and anisole.

**MW Averages**  
 Mp: 78699 Mn: 41599 Mv: 89656 Mw: 100651  
 Mz: 194273 Mz+1: 300882 PD: 2.4196

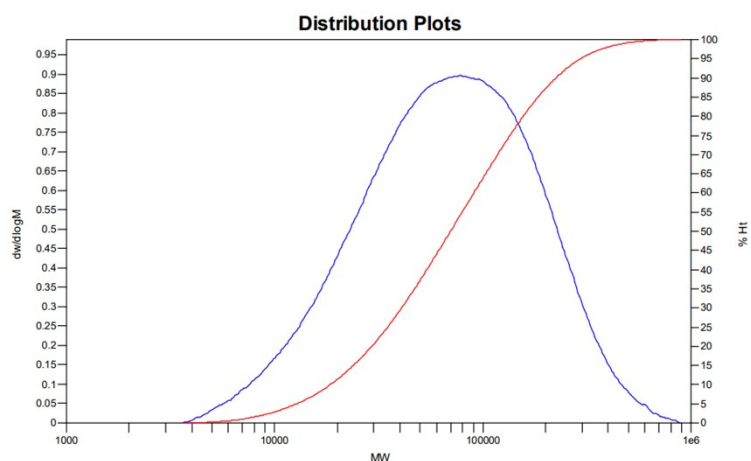


**Fig. S3.** The GPC trace of PBNT-TzTz recorded at 140 °C with 1,2,4-trichlorobenzene as eluent.

**Table S5.** The solubility of the polymers in anisole at room temperature.

Polymer	D18	PM6	PTQ10	PBDT-TzTz	PTTz-3HD	PBNT-TzTz
$M_n$ (kDa)	45	47	32	43	54	42
Solubility (mg mL <sup>-1</sup> )	<0.1	<0.1	<0.1	<0.1	<0.1	11.2

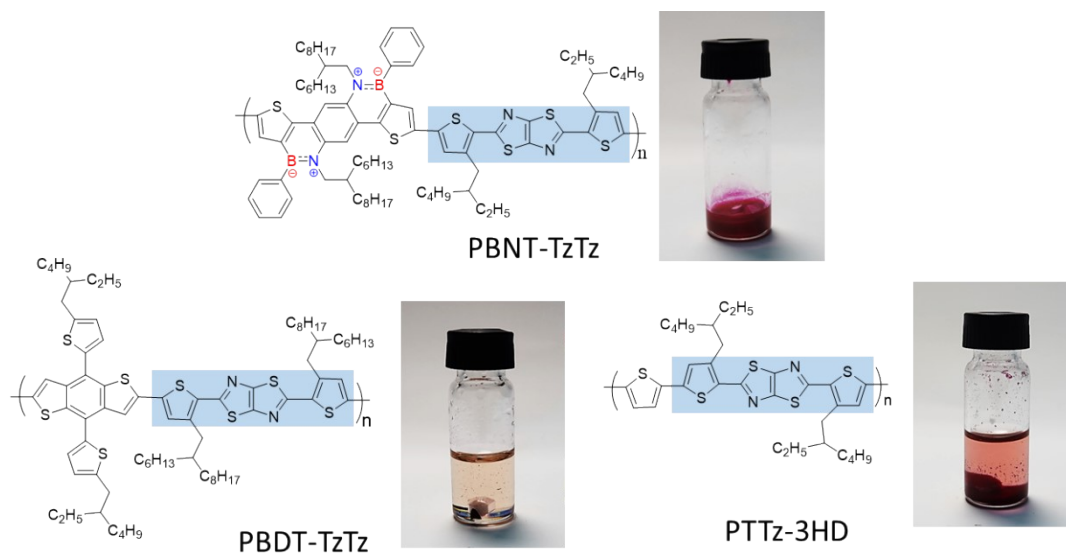


**Fig. S4.** Photographs of PBNT-TzTz, PBDT-TzTz, and PTTz-3HD in anisole.

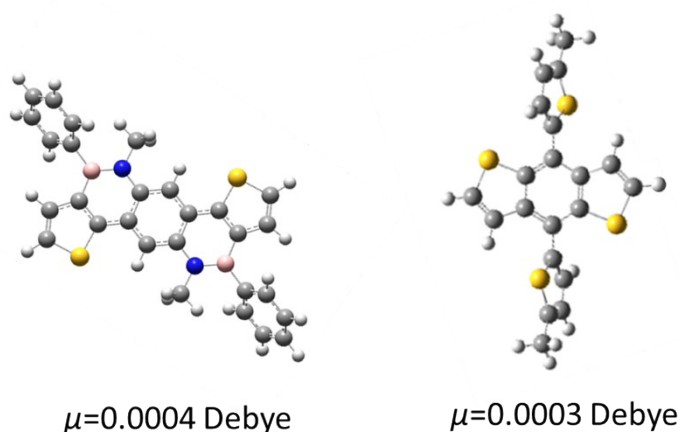


**Fig. S5.** The dipole moment of BNT (left) and BDT (right) calculated at the B3LYP/6-31+G\* level.

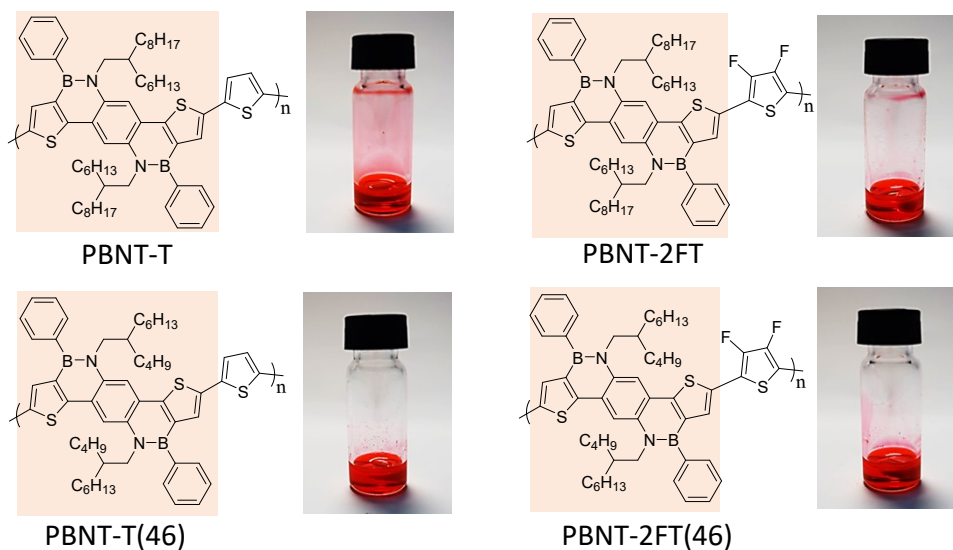


**Fig. S6.** Photographs of the other BNT-based polymers in anisole at the concentration of 8 mg mL<sup>-1</sup>.

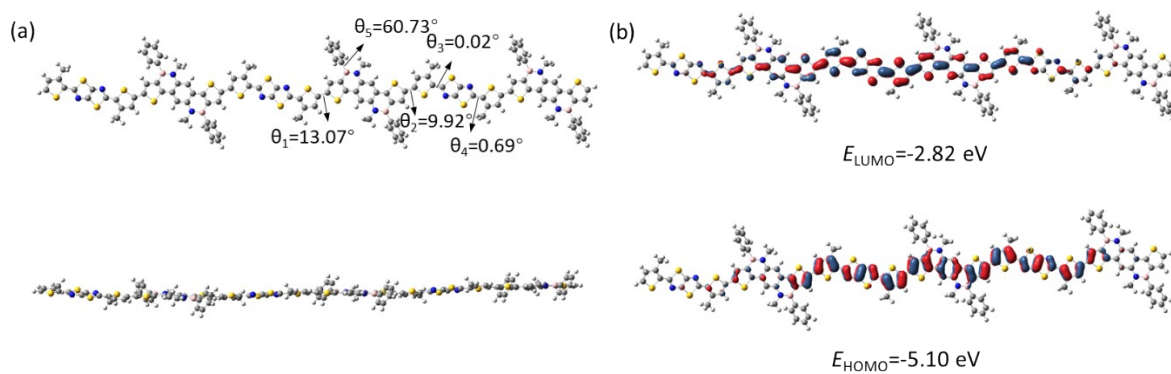


**Fig. S7.** DFT calculation results based on three repeat units of PBNT-TzTz at the B3LYP/6-31+G\* level. (a) Optimized molecular geometries. (b) Calculated molecular orbitals.

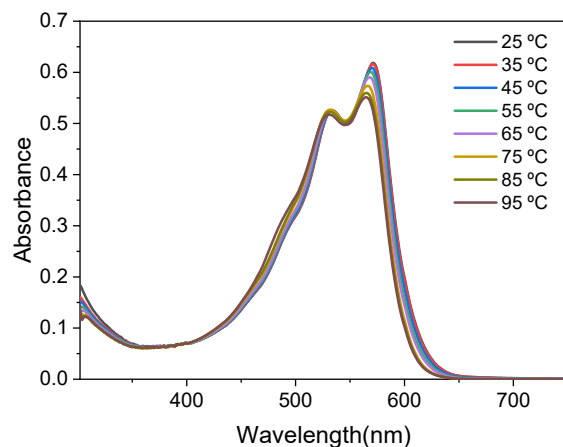


**Fig. S8.** Temperature-dependent UV-vis absorption spectra of PBNT-TzTz in anisole solution ( $1.0 \times 10^{-5}$  M).

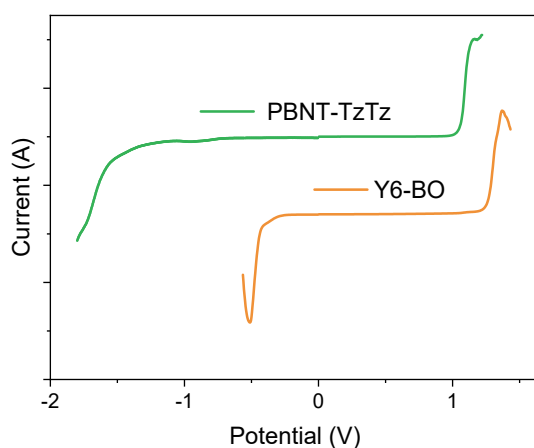


**Fig. S9.** Square wave voltammograms of PBNT-TzTz and Y6-BO.  $E_{\text{LUMO/HOMO}} = -(5.13 + E_{\text{ox/te}} - E_{\text{Fc/Fc}^+})$  eV and  $E_{\text{Fc/Fc}^+} = 0.63$  eV.

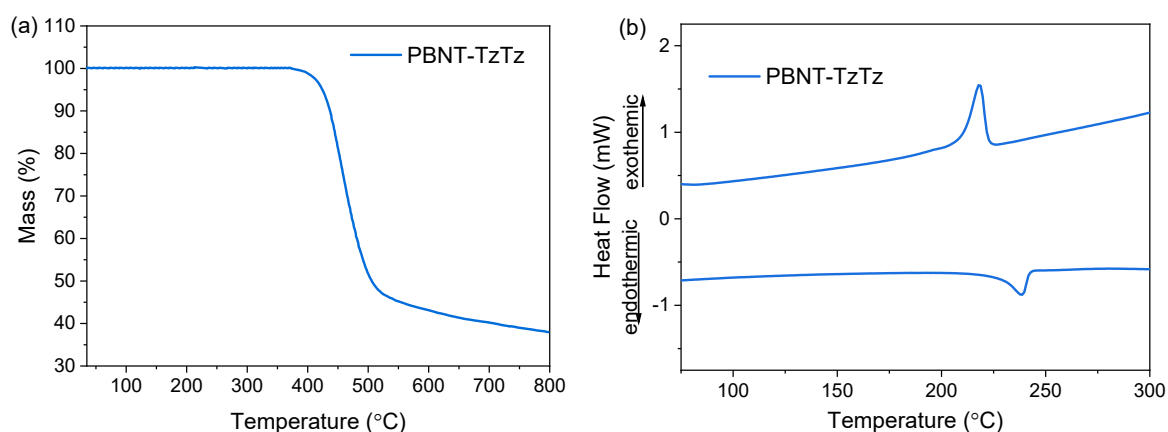


**Fig. S10.** Thermal properties of the polymer PBNT-TzTz. (a) The TGA plots. (b) The DSC traces.

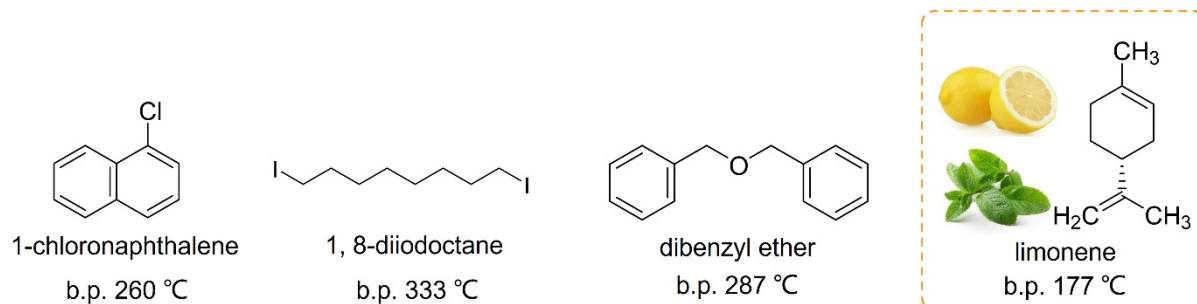


**Fig. S11.** The chemical structures and boiling points of commonly used solvent additives and limonene.

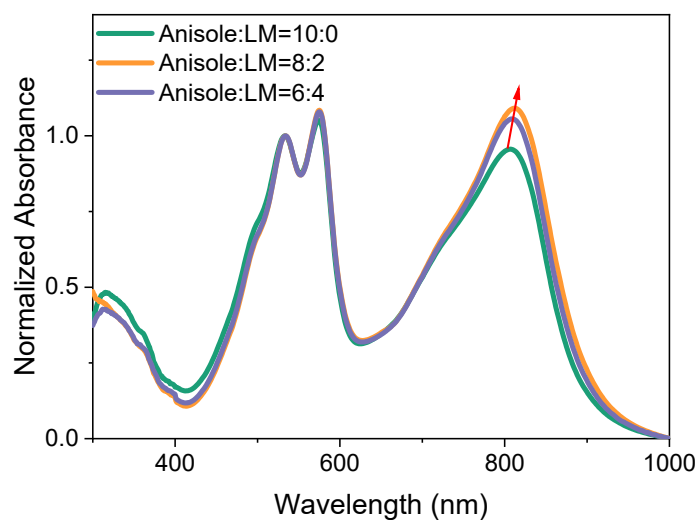


**Fig. S12.** Normalized absorption spectra of the PBNT-TzTz:Y6-BO blend films processed from different Anisole:LM solvent mixtures.

**Table S6.** The device parameters of the OSCs based on PBNT-TzTz:Y6-BO blend under AM1.5G irradiation at 100 mW cm<sup>-2</sup>.

D/A ratio	Solvent (v:v)	TA	$V_{oc}$ (V)	$J_{sc}$ (mA cm <sup>-2</sup> )	FF (%)	PCE (%)
1:1.2	Anisole:LM=10:0	/	0.88	24.18	63.5	13.52
1:1.2	Anisole:LM=8:2	100 °C 10 min	0.88	25.40	70.0	15.65
1:1			0.86	24.65	67.3	14.27
1:1.5			0.88	23.97	65.1	13.73
			60 °C 10 min	0.87	24.96	66.7
	Anisole:LM=8:2	80 °C 10 min	0.88	25.13	68.3	15.10
1:1.2		120 °C 10 min	0.88	25.25	68.6	15.24
	Anisole:LM=6:4		0.88	24.64	66.9	14.51
	Anisole:LM=4:6	100 °C 10 min	0.88	24.66	62.3	13.52
	Anisole:LM=2:8		0.87	23.62	58.0	11.95
	Anisole:LM=0:10		0.87	22.26	54.7	10.59

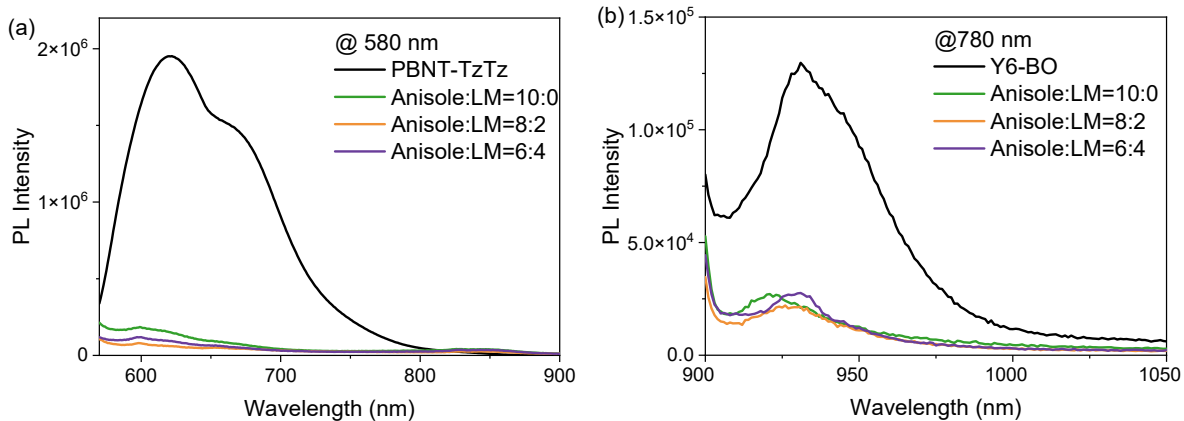


**Fig. S13.** The photoluminescence spectra of PBNT-TzTz, Y6-BO, and the blends. (a) PBNT-TzTz and the PBNT-TzTz:Y6-BO blend films processed from different solvents with excitation wavelength at 580 nm. (b) Y6-BO and the PBNT-TzTz:Y6-BO blend films processed from different solvents with excitation wavelength at 780 nm.

**Table S7.** The quenching efficiency of the PBNT-TzTz:Y6-BO blend films.

Solvent	$\Delta PL_D^a$	$\Delta PL_A^b$
Anisole:LM=10:0	90.5%	80.5%
Anisole:LM=8:2	95.4%	85.3%
Anisole:LM=6:4	93.3%	81.5%

$$^a \Delta PL_D = \frac{1 - PL_{blend}}{PL_{donor}} ; \quad ^b \Delta PL_A = \frac{1 - PL_{blend}}{PL_{acceptor}}$$

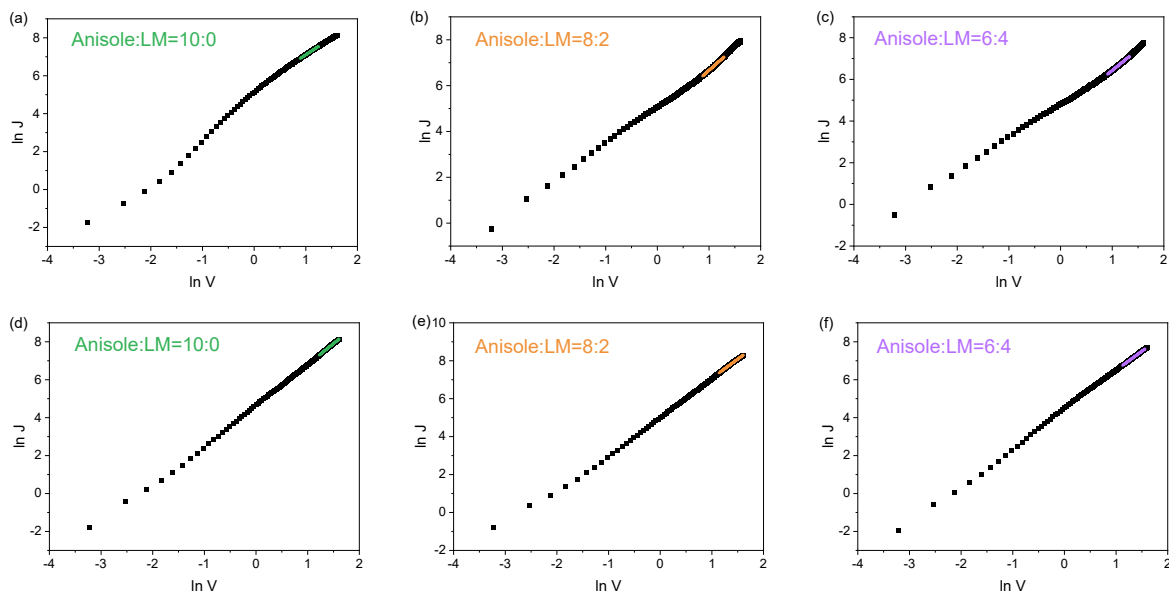


**Fig. S14.** The  $J-V$  curves of the single-carrier devices based on the PBNT-TzTz:Y6-BO blends processed from different solvents. (a–c) The hole-only devices. (d–f) The electron-only devices.

**Table S8.** The mobilities of the PBNT-TzTz:Y6-BO blend films acquired from single-carrier devices.

Solvent	$\mu_e$ (cm <sup>2</sup> V <sup>-1</sup> s <sup>-1</sup> )	$\mu_h$ (cm <sup>2</sup> V <sup>-1</sup> s <sup>-1</sup> )
Anisole:LM=10:0	$7.72 \times 10^{-4}$	$9.97 \times 10^{-4}$
Anisole:LM=8:2	$1.19 \times 10^{-3}$	$1.51 \times 10^{-3}$
Anisole:LM=6:4	$9.15 \times 10^{-4}$	$1.22 \times 10^{-3}$

**Table S9.** The exciton dissociation probability of the PBNT-TzTz:Y6-BO blend films.

Solvent	$P(E, T)$
Anisole:LM=10:0	95.3%
Anisole:LM=8:2	97.6%
Anisole:LM=6:4	95.8%

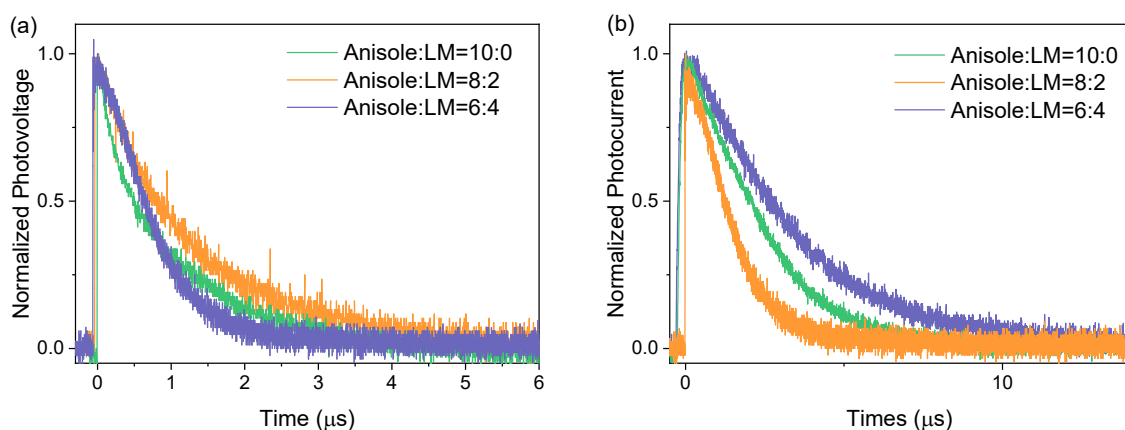


**Fig. S15.** (a) Transient photovoltage and (b) transient photocurrent of the OSCs based on PBNT-TzTz:Y6-BO processed from anisole:LM solvent mixtures.

**Table S10.** The charge carrier lifetime and decay times in the PBNT-TzTz:Y6-BO devices.

Solvent	Charge carrier lifetime (μs)	Charge carrier decay time (μs)
Anisole:LM=10:0	0.72	2.63
Anisole:LM=8:2	0.77	1.53
Anisole:LM=6:4	0.59	3.53

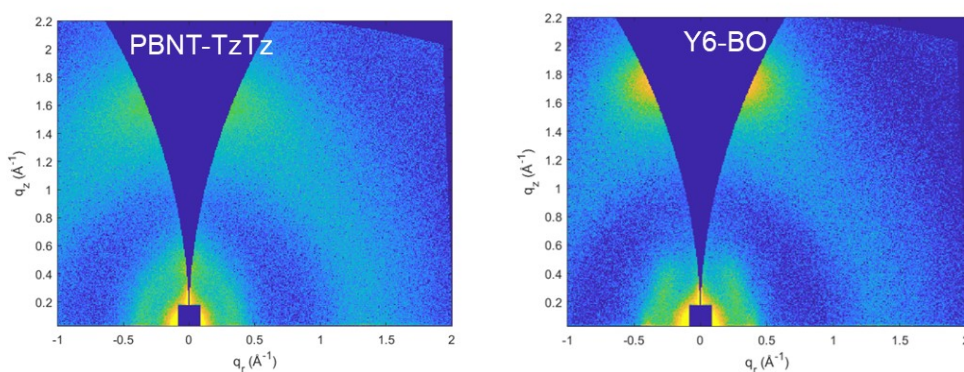


**Fig. S16.** The 2D-GIWAXS patterns of the neat PBNT-TzTz and Y6-BO films.

**Table S11.** Characteristic length scale of the neat PBNT-TzTz and Y6-BO films measured by GIWAXS.

Film	$\pi$ - $\pi$ stacking (010)			Lamellar stacking (100)		
	$q$ ( $\text{\AA}^{-1}$ )	$d$ -spacing ( $\text{\AA}$ )	CCL ( $\text{\AA}$ )	$q$ ( $\text{\AA}^{-1}$ )	$d$ -spacing ( $\text{\AA}$ )	CCL ( $\text{\AA}$ )
PBNT-TzTz	1.68	3.74	16.44	0.35	17.94	NA
Y6-BO	1.77	3.55	19.63	0.28	22.27	53.42

**Table S12.** Characteristic length scale of the PBNT-TzTz: Y6-BO blend films measured by GIWAXS.

Film	$\pi$ - $\pi$ stacking (010)			Lamellar stacking (100)		
	$q$ ( $\text{\AA}^{-1}$ )	$d$ -spacing ( $\text{\AA}$ )	CCL ( $\text{\AA}$ )	$q$ ( $\text{\AA}^{-1}$ )	$d$ -spacing ( $\text{\AA}$ )	CCL ( $\text{\AA}$ )
Anisole:LM=10:0	1.73	3.63	12.71	0.37	16.97	35.89
Anisole:LM=8:2	1.73	3.63	15.28	0.36	17.44	36.30
Anisole:LM=6:4	1.73	3.63	14.81	0.37	16.97	36.30

**Table S13.** Summary for reported OSCs processed from eco-compatible solvents.<sup>a</sup>

Solvent	Active layer	$V_{oc}$ (V)	$J_{sc}$ ( $\text{mA cm}^{-2}$ )	FF	PCE (%)	Reference
2-MA	PBDT-TS1:PC <sub>71</sub> BM	0.79	17.39	0.70	9.67	12
Anisole	PBDT-TS1:PPDIODT	0.76	14.67	0.49	5.43	13
Anisole	PB3T:IT-M	1.00	18.9	0.63	11.9	14
Water/Ethanol	PPDT2FBT-A:PC <sub>61</sub> BO <sub>12</sub>	0.76	5.08	0.53	2.05	15
2-MA	PffBT-RT4:PC <sub>71</sub> BM	0.71	17.40	0.71	8.84	16
2-MA	asy-BTBDTs:PC <sub>71</sub> BM	0.80	10.4	69.7	5.70	17
2-MA	PTB7-Th:PC <sub>71</sub> BM	0.78	16.9	0.72	9.50	18
Water/Ethanol	PPDT2FBT-A:PC <sub>71</sub> BO <sub>15</sub>	0.75	6.23	0.54	2.51	19
Water/Ethanol	PFO:PCBO-12-AM	0.60	6.14	0.61	2.25	20
Anisole/LM	PBNT-TzTz:Y6-BO	0.88	25.40	0.70	15.65	This work

<sup>a</sup> 2-MA represents 2-methylanisole; LM represents limonene.

## Reference

- [1] S. Pang, Z. Wang, X. Yuan, L. Pan, W. Deng, H. Tang, H. Wu, S. Chen, C. Duan, F. Huang and Y. Cao, *Angew. Chem. Int. Ed.* 2021, **60**, 8813.
- [2] I. Osaka, R. Zhang, G. Sauvé, D.-M. Smilgies, T. Kowalewski and R. D. McCullough, *J. Am. Chem. Soc.* 2009, **131**, 2521.
- [3] B. Yin, Z. Chen, S. Pang, X. Yuan, Z. Liu, C. Duan, F. Huang and Y. Cao, *Adv. Energy Mater.* 2022, **12**, 2104050.
- [4] R. E. M. Willems, C. H. L. Weijtens, X. de Vries, R. Coehoorn and R. A. J. Janssen, *Adv. Energy Mater.* 2019, **9**, 1803677.
- [5] J. G. Osteryoung and R. A. Osteryoung, *Anal. Chem.* 1985, **57**, 101.
- [6] M. J. Frisch, G. W. Trucks, H. B. Schlegel, G. E. Scuseria, M. A. Robb, J. R. Cheeseman, G. Scalmani, V. Barone, B. Mennucci, G. A. Petersson, H. Nakatsuji, M. Caricato, X. Li, H. P. Hratchian, A. F. Izmaylov, J. Bloino, G. Zheng, J. L. Sonnenberg, M. Hada, M. Ehara, K. Toyota, R. Fukuda, J. Hasegawa, M. Ishida, T. Nakajima, Y. Honda, O. Kitao, H. Nakai, T. Vreven, J. A. Montgomery, J. E. Peralta, F. Ogliaro, M. Bearpark, J. J. Heyd, E. Brothers, K. N. Kudin, V. N. Staroverov, R. Kobayashi, J. Normand, K. Raghavachari, A. Rendell, J. C. Burant, S. S. Iyengar, J. Tomasi, M. Cossi, N. Rega, J. M. Millam, M. Klene, J. E. Knox, J. B. Cross, V. Bakken, C. Adamo, J. Jaramillo, R. Gomperts, R. E. Stratmann, O. Yazyev, A. J. Austin, R. Cammi, C. Pomelli, J. W. Ochterski, R. L. Martin, K. Morokuma, V. G. Zakrzewski, G. A. Voth, P. Salvador, J. J. Dannenberg, S. Dapprich, A. D. Daniels, O. Farkas, J. B. Foresman, J. V. Ortiz, J. Cioslowski and D. J. Fox, *Gaussian-09, Revision A.02*, Wallingford CT.
- [7] J. C. Blakesley, F. A. Castro, W. Kylberg, G. F.A. Dibb, C. Arantes, R. Valaski, M. Cremona, J. S. Kim and J. Kim, *Org. Electron.* 2014, **15**, 1263.
- [8] F. Campana, C. Kim, A. Marrocchi and L. Vaccaro, *J. Mater. Chem. C* 2020, **8**, 15027.
- [9] D. Prat, A. Wells, J. Hayler, H. Sneddon, C. Robert McElroy, S. Abou-Shehadad and P. J. Dunn, *Green Chem.* 2016, **18**, 288.
- [10] D. Prat, O. Pardigon, H.-W. Flemming, S. Letestu, Ve. Ducandas, P. Isnard, E. Guntrum, T. Senac, S. Ruisseau, P. Cruciani and P. Hosek, *Org. Process Res. Dev.* 2013, **17**, 1517.
- [11] R. K. Henderson, C. Jiménez-González, D. J. C. Constable, S. R. Alston, G. G. A. Inglis, G. Fisher, J. Sherwood, S. P. Binks and A. D. Curzons, *Green Chem.* 2011, **13**, 854.
- [12] H. Zhang, H. Yao, W. Zhao, L. Ye and J. Hou, *Adv. Energy Mater.* 2016, **6**, 1502177.
- [13] S. Li, H. Zhang, W. Zhao, L. Ye, H. Yao, B. Yang, S. Zhang and J. Hou, *Adv. Energy Mater.* 2016, **6**, 1501991.

- [14] D. Liu, B. Yang, B. Jang, B. Xu, S. Zhang, C. He, H. Y. Woo and J. Hou, *Energy Environ. Sci.* 2017, **10**, 546.
- [15] C. Lee, H. R. Lee, J. Choi, Y. Kim, T. Luan Nguyen, W. Lee, B. Gautam, X. Liu, K. Zhang, F. Huang, J. H. Oh, Han Y. Woo and B. J. Kim, *Adv. Energy Mater.* 2018, **8**, 1802674
- [16] S. Y. Son, J. W. Kim, J. H. Lee, G.-W. Kim, J. Hong, J. Y. Kim and T. Park, *J. Mater. Chem. A* 2018, **6**, 24580.
- [17] J. Lee, T. H. Lee, M. M. Byranvand, K. Choi, H. I. Kim, S. A. Park, J. Y. Kim and T. Park, *J. Mater. Chem. A* 2018, **6**, 5538.
- [18] K. Zhang, Z. Chen, A. Armin, S. Dong, R. Xia, H.-L. Yip, S. Shoaee, F. Huang and Y. Cao, *Sol. RRL* 2018, **2**, 1700169.
- [19] C. Kim, H. Kang, N. Choi, S. Lee, Y. Kim, J. Kim, Z. Wu, H. Y. Woo and B. J. Kim, *J. Mater. Chem. C* 2020, **8**, 15224.
- [20] L. Shang, W. Zhang, B. Zhang, Y. Gao, S. He, G. Dong, W. Li, H. Bai, G. Yue, S. Chen and F. Tan, *Sol. RRL* 2022, DOI: 10.1002/solr.202200605.